Ketene-forming eliminations from aryl phenylacetates promoted by R_2NH in MeCN. Origin of the curved Hammett plot

Bong Rae Cho,* Nam Soo Kim, Yong Kwan Kim and Kyung Hwa Son

Department of Chemistry, Korea University, 1-Anamdong, Seoul 136-701, Korea

Received (in Cambridge, UK) 9th March 2000, Accepted 14th April 2000
Published on the Web 23rd May 2000

Elimination reactions of $YC_6H_4CH_2C(O)OC_6H_3$-2-X-4-NO_2 promoted by R_2NH in MeCN have been studied kinetically. The reactions are second-order and exhibit Brønsted $\beta = 0.52$–0.87, $|\beta_{lg}| = 0.37$–0.65, and $\rho_H = 1.9$–4.1. The β and ρ_H values decrease as the leaving group becomes less basic and the $|\beta_{lg}|$ values decrease with a stronger base. The results are interpreted in terms of an E1cb-like transition state with extensive C_β–H bond cleavage, significant negative charge development at the β-carbon, and limited C_α–OAr bond cleavage. For all reactions, the Hammett plots are curvilinear and show downward curvature. The curvature is more pronounced as the leaving group becomes poorer. The results have been attributed to the highly carbanionic transition state, which is moved towards the reactant on the horizontal reaction coordinate by a stronger electron-withdrawing substituent.

Base-catalyzed hydrolysis of aryl *p*-nitrophenylacetates and other activated esters have been known to proceed by an E1cb mechanism to afford the ketene intermediate followed by the addition of water under various conditions.[1–13] When the reaction condition was changed from OH^- in H_2O to R_2NH in MeCN or $R_2NH/R_2NH_2^+$ in 70% MeCN(aq), the mechanism changed to E2.[14,15] Competing E2 and E1cb mechanisms were noted in elimination reactions from *p*-nitrophenyl *p*-nitrophenylacetate promoted by $R_2NH/R_2NH_2^+$ in 70% MeCN(aq).[14]

An interesting observation from the previous study was the concave downward Hammett plots in R_2NH-promoted eliminations from *p*-nitrophenyl arylacetates and 2,4-dinitrophenyl arylacetates.[14] The rate data could be correlated with eqn. (1),

$$\log (k/k_o) = \rho_H\sigma^- + \tau(\sigma^-)^2 = (\rho_H + \tau\sigma^-)\,\sigma^- \qquad (1)$$

where ρ_H and τ are the slope of the Hammett plot when the β-aryl substituent is H and the proportionality factor by which the ρ value is influenced by the electron-withdrawing ability of the substituents, respectively. However, due to the lack of sufficient data, the origin of the curved Hammett plot could not be clearly elucidated.

Curved Hammett plots had been previously reported for elimination reactions that proceed *via* E1-like transition states. For the ethanethiolate-catalyzed elimination reaction of benzyldimethylmethyl chloride in methanol, *tert*-butoxide-promoted elimination from 1-arylethyl chloride in 90% *tert*-BuOH–10% DMSO, and the acetate-catalyzed elimination reaction of *threo*-3-chloro-3-(4-substituted phenyl)-1,2-diphenylpropan-1-one in a 4 : 1 DMSO–MeOH solvent, the slopes of the Hammett plots changed from a negative value to a positive one with a distinct minimum.[16–18] The results were interpreted in terms of the change in the charge character of the E2 transition state from one with net positive charge to one with net negative charge as the β-aryl substituent was made more electron-withdrawing. However, the concave downward Hammett plot observed in the ketene-forming reactions had no precedent in elimination reactions.

In this work, we studied the reactions of aryl arylacetates **2**–**4** with R_2NH in MeCN (eqn. (2)). The mechanism and structure–reactivity relationship in the ketene-forming elimination reactions have been determined. When combined with the existing data for **1** and **5**, the results establish the origin of the concave downward curvature observed in the Hammett plot for the ketene-forming elimination reactions.

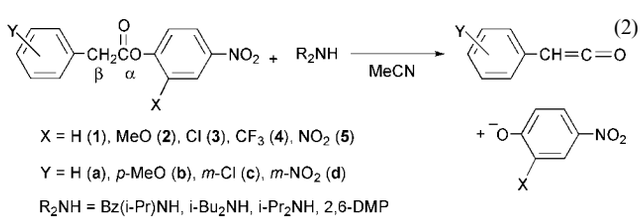

(2)

Results

Aryl arylacetates **2**–**4** were synthesized by the reaction between substituted phenylacetic acid, substituted phenols, 2-chloro-1-methylpyridinium iodide, and Et_3N in CH_2Cl_2 as described previously.[14,19] The products of the reactions of **1a** and **5a** with diisopropylamine were identified as *N*,*N*-diisopropylbenzamide and aryloxides.[14] For reactions of **2**–**4** with R_2NH in MeCN, the yields of aryloxides as determined by comparison of the UV absorption of the infinity sample of the kinetic runs with those of the authentic samples were in the range 90–98%. The possibility of a competing aminolysis had been ruled out by a previous study.[14]

The rates of reactions between **2**–**4** and R_2NH in MeCN were followed by monitoring the increase in the absorption of the aryloxides at 400–450 nm with a UV–vis spectrophotometer as described previously.[14] In all cases, clean isosbestic points were noted in the range 292–298 nm. Excellent pseudo-first-order kinetic plots, which covered at least 3 half-lives, were obtained. Dividing the pseudo-first-order rate constants by the base concentration provided the second-order rate coefficients k_2 presented in Table 1.

The k_2 values for eliminations from **2** showed excellent correlation with the pK_a values of the promoting bases on the Brønsted plot (Fig. 1). Similar plots were obtained for the reactions of **3** and **4** (plots not shown). Table 2 summarizes the β values for the ketene-forming elimination reactions from **1**–**5**. The β values are in the range 0.52–0.87. The value decreases with a stronger electron-withdrawing β-aryl substituent and a better leaving group.

DOI: 10.1039/b001929l

This journal is © The Royal Society of Chemistry 2000

Table 1 Rate constants for ketene-forming elimination from $YC_6H_4CH_2CO_2Ar$[a] promoted by R_2NH in MeCN at 25.0 °C

		$k_2/10^{-2}$ M^{-1} s^{-1}[b]											
Base[c]	pK_a[d]	**2a**	**2b**	**2c**	**2d**	**3a**	**3b**	**3c**	**3d**	**4a**	**4b**	**4c**	**4d**
Bz(i-Pr)NH	16.8	0.0724	0.00851	1.29	8.13	1.58	0.288	21.6	121	6.17	1.41	53.8	309
i-Bu_2NH	18.2	1.07	0.145	15.4	81.1	17.3	3.72	187	873	53.1	14.6	443	2240
i-Pr_2NH	18.5	1.91	0.257	28.4	136	29.0	6.46	300	1380	105	25.7	708	3550
2,6-DMP[e]	18.9	4.17	0.575	57.9	267	58.7	12.7	566	2510	213	56.2	1170	5890

[a] [Substrate] = 2.0×10^{-5} M. [b] Estimated uncertainty, ±5%. [c] [Base] = 1.0×10^{-3}–10^{-1} M. [d] Ref. 14. [e] *cis*-2,6-Dimethylpiperidine.

Table 2 Effect of aryl substituents upon Brønsted β values for eliminations from $YC_6H_4CH_2CO_2C_6H_3$-2-X-4-NO_2 promoted by R_2NH in MeCN at 25.0 °C

	β				
Y	X = H[a]	X = MeO	X = Cl	X = CF_3	X = NO_2[a]
p-CH_3O	0.84 ± 0.01	0.87 ± 0.01	0.79 ± 0.01	0.75 ± 0.03	0.72 ± 0.02
H	0.82 ± 0.01	0.84 ± 0.01	0.75 ± 0.01	0.73 ± 0.05	0.69 ± 0.04
m-Cl	0.81 ± 0.02	0.78 ± 0.02	0.67 ± 0.01	0.64 ± 0.02	0.56 ± 0.02
m-NO_2	0.68 ± 0.03	0.72 ± 0.01	0.63 ± 0.01	0.61 ± 0.01	0.52 ± 0.02

[a] Ref. 14.

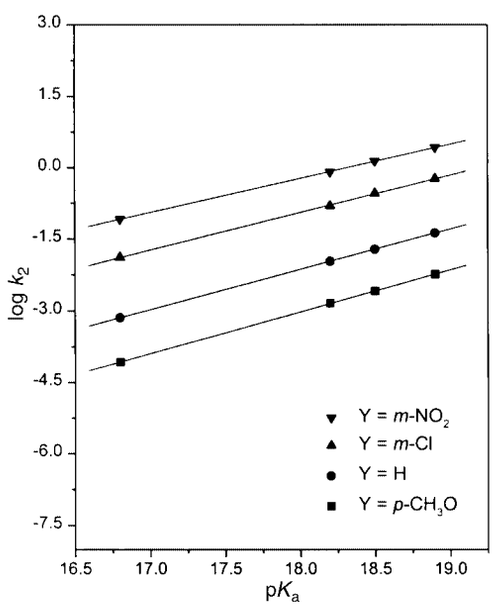

Fig. 1 Brønsted plots for the ketene-forming eliminations from $YC_6H_4CH_2CO_2C_6H_3$-2-MeO-4-NO_2 promoted by R_2NH in MeCN at 25.0 °C.

The Brønsted plots for Bz(i-Pr)NH-promoted eliminations from $YC_6H_4CH_2CO_2Ar$ with the leaving group variations are shown in Fig. 2. The plots for other amine bases are similar but are omitted for brevity. In all cases, the rate data for **1** showed positive deviation from the plots, probably because of the leaving group steric effect. Since the *p*-nitrophenoxide in **1** is the only leaving group without an *ortho* substituent, it should be sterically less hindered than other substrates, to increase the rate. Although the steric effects of the *ortho* substituents in **2**–**4** may not be identical, the difference would be smaller than that between **1** and **2**–**4**. Therefore, the $|\beta_{lg}|$ values were calculated without the data for **1**, by assuming that the rates of eliminations from **2**–**4** are primarily influenced by the electronic effects. The $|\beta_{lg}|$ values are summarized in Table 3. The values are in the range 0.37–0.65 and decrease as the electron-withdrawing ability of the β-aryl substituent and the pK_a value of the promoting base are increased.

The Hammett plots for R_2NH-promoted elimination from **2a**–**d** are curvilinear and show downward curvature (Fig. 3).

Table 3 Effect of aryl substituents upon Brønsted β_{lg} values for eliminations from $YC_6H_4CH_2CO_2C_6H_3$-2-X-4-NO_2 promoted by R_2NH in MeCN at 25.0 °C

	$\lvert\beta_{lg}\rvert$			
R_2NH	Y = *p*-CH_3O	Y = H	Y = *m*-Cl	Y = *m*-NO_2
Bz(i-Pr)NH	0.65 ± 0.03	0.55 ± 0.02	0.48 ± 0.02	0.45 ± 0.01
i-Bu_2NH	0.60 ± 0.04	0.52 ± 0.03	0.42 ± 0.01	0.40 ± 0.01
i-Pr_2NH	0.58 ± 0.02	0.50 ± 0.01	0.39 ± 0.01	0.38 ± 0.01
2,6-DMP[a]	0.58 ± 0.01	0.48 ± 0.01	0.38 ± 0.02	0.37 ± 0.01

[a] *cis*-2,6-Dimethylpiperidine.

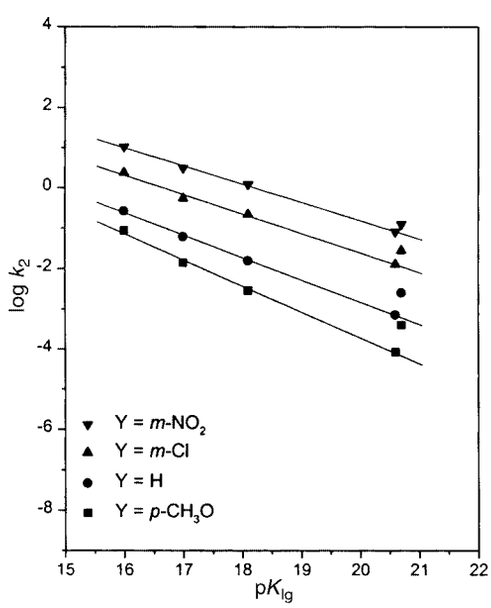

Fig. 2 Brønsted plots for the ketene-forming eliminations from $YC_6H_4CH_2CO_2C_6H_3$-2-X-4-NO_2 promoted by Bz(i-Pr)NH in MeCN at 25.0 °C.

Similar plots were observed for the reactions of **3** and **4** (plots not shown). Utilizing a nonlinear regression analysis program, the values of ρ_H and τ that best fit with eqn. (1) have been calculated.[20] The ρ_H and $|\tau|$ values are in the ranges 1.9–4.1 and 0.2–2.3, respectively (Table 4). For a given leaving group, the

Table 4 Effect of base strength upon the ρ_H and τ values for eliminations from $YC_6H_4CH_2CO_2C_6H_3$-2-X-4-NO_2 promoted by R_2NH in MeCN at 25.0 °C

	X = H [b]		X = MeO		X = Cl		X = CF_3		X = NO_2 [b]	
Base	ρ_H	τ	ρ_H	τ	ρ_H	τ	ρ_H	τ	ρ_H	τ
Bz(i-Pr)NH	3.5 ± 0.1	−1.6 ± 0.2	4.1 ± 0.1	−1.7 ± 0.2	3.5 ± 0.1	−1.2 ± 0.1	2.9 ± 0.1	−0.7 ± 0.2	2.6 ± 0.2	−0.5 ± 0.3
i-Bu_2NH	3.6 ± 0.1	−2.3 ± 0.1	3.9 ± 0.1	−1.7 ± 0.2	3.2 ± 0.1	−1.1 ± 0.1	2.7 ± 0.1	−0.6 ± 0.1	2.0 ± 0.2	−0.2 ± 0.3
i-Pr_2NH	3.3 ± 0.1	−1.9 ± 0.1	3.9 ± 0.1	−1.8 ± 0.1	3.1 ± 0.1	−1.0 ± 0.1	2.7 ± 0.2	−0.7 ± 0.3	2.0 ± 0.2	−0.3 ± 0.3
2,6-DMP [a]	3.6 ± 0.1	−2.3 ± 0.1	3.8 ± 0.1	−1.8 ± 0.1	3.1 ± 0.1	−1.1 ± 0.1	2.4 ± 0.2	−0.5 ± 0.2	1.9 ± 0.1	−0.2 ± 0.1

[a] *cis*-2,6-Dimethylpiperidine. [b] Calculated from the data in ref. 14.

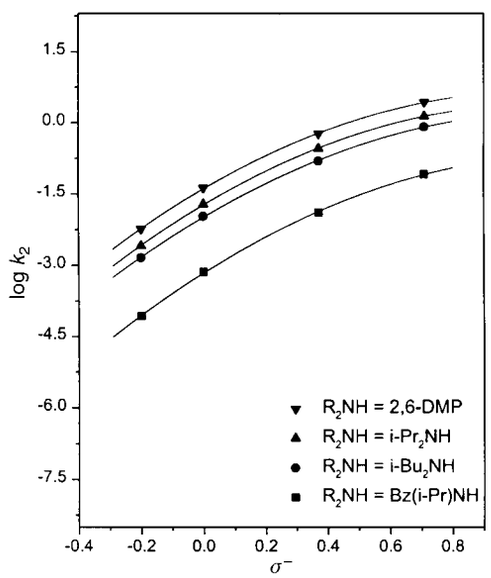

Fig. 3 Hammett plots for the ketene-forming eliminations from $YC_6H_4CH_2CO_2C_6H_3$-2-MeO-4-NO_2 promoted by R_2NH in MeCN at 25.0 °C.

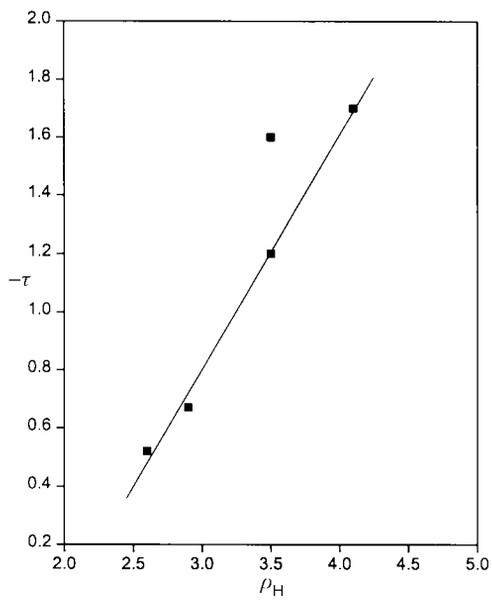

Fig. 4 Plot of $-\tau$ *vs.* ρ_H for the ketene-forming eliminations from $YC_6H_4CH_2CO_2C_6H_3$-2-X-4-NO_2 promoted by Bz(i-Pr)NH in MeCN at 25.0 °C.

values are nearly the same regardless of the base strength. On the other hand, both values increase, as the leaving group is made poorer. Fig. 4 shows the plot of $|\tau|$ *vs.* ρ_H for Bz(i-Pr)NH-promoted eliminations from **1**–**5**. The plot is linear, if the positive deviation for **1** is excluded. Similar plots were obtained with other amine bases (plots not shown).

Discussion

Mechanism and transition state structure for eliminations from 1–5 promoted by R_2NH in MeCN

It was previously established that the ketene-forming eliminations from **1** and **5** promoted by R_2NH in MeCN proceed by the E2 mechanism.[14] Results of kinetic investigations and product studies reveal that the reactions of **2**–**4** with R_2NH in MeCN also proceed by the same E2 mechanism. Since the reactions exhibited second-order kinetics, all but bimolecular pathways can be ruled out. In addition, an E1cb mechanism is negated by the substantial values of β and $|\beta_{lg}|$.[21–24]

The structures of the transition states may be assessed by the Brønsted β, Hammett ρ, and β_{lg} values. The Brønsted β values indicate the extent of proton transfer in the transition state. For R_2NH-promoted eliminations from **1**–**5**, values of $\beta = 0.52$–0.87 were determined (Table 2). This indicates moderate to extensive cleavage of the C_β–H bonds in the transition states.

The β_{lg} values are usually taken as a measure of the extent of the leaving group cleavage. However, it should be noted that the values of $|\beta_{lg}|$ are not restricted to 0–1. In fact, for reactions involving loss of arenesulfonate in the rate-determining step, they range up to nearly 3.[25] For ketene-forming eliminations from aryl *p*-nitrophenylacetates, the maximum value of $|\beta_{lg}| = 1.34$ was reported.[14,26] These variations indicate that the equilibrium proton acidity of the leaving groups, as measured by pK_a, is not a proper model for the kinetic behavior of the same leaving groups when they ionically cleave from a more complex molecule.[27] Therefore, they should be taken as a qualitative measure of the extent of leaving group departure in the transition state. For eliminations from **1**–**5** promoted by R_2NH in MeCN, $|\beta_{lg}|$ values of 0.37–0.65 have been determined (Table 3). Since the $|\beta_{lg}| = 0.4$–0.5 values observed for the R_2NH-promoted elimination from **1** were previously interpreted in terms of an E1cb-like transition state,[14] the present results can most reasonably be ascribed to a limited extent of C_α–OAr bond cleavage in the transition state.

The extent of negative charge development in the transition state may be estimated with the Hammett ρ values. For all reactions the Hammett plots are curvilinear and show downward curvature (Fig. 3). The origin of the curvature will be discussed below. However, the ρ_H value, which is the slope of the Hammett plot when Y = H, can be used as a measure of the negative charge character of the transition state (Table 4). Hence, the values of $\rho_H = 1.9$–4.1 obtained for the ketene-forming elimination reactions can be interpreted in terms of significant negative charge development at the β-carbon in the transition state.

The combined results reveal that the R_2NH-promoted ketene-forming eliminations from **1**–**5** proceed by the concerted E2 mechanism with extensive C_β–H bond cleavage, significant negative charge development at the β-carbon, and limited C_α–OAr bond cleavage.

Origin of the curved Hammett plot in the ketene-forming eliminations

Curved Hammett plots have been previously observed in substitution, elimination, acyl transfer, and oxidation reactions.[16–18,28–30] Causes of such curvature have been attributed to (i) the change in mechanism, (ii) a single mechanism with a different extent of bond formation and cleavage, or a change of the charge character, in the transition state, and (iii) a different balance of polar and resonance effects by different substituents in the transition state.

The origin of the downward curvature observed in the Hammett plots for the ketene-forming eliminations from **1**–**5** can be attributed to the possibility (ii). Since the reactions proceed by a common E2 mechanism, possibility (i) can be ruled out. Possibility (iii) can also be negated because the downward curvature is caused by the stronger electron-withdrawing groups, not by the electron-donating groups such as *p*-MeO, which is the only *para* substituent employed in this study that may cause such an effect. On the other hand, the result can readily be interpreted in terms of a gradual decrease in the transition state carbanionic character with a stronger electron-withdrawing β-aryl substituent. Because the ketene-forming elimination is assumed to proceed *via* an E1cb-like transition state on the horizontal reaction coordinate, the transition state would be shifted toward the reactant by a stronger electron-withdrawing β-aryl substituent, to decrease the extent of negative charge development. The transition state would not be stabilized as effectively by the substituent as when there is no such effect. Hence, the rates of eliminations from such substrates would become slower than expected from the substituent effect, which would in turn cause a downward curvature in the Hammett plot. Furthermore, this effect would be more pronounced for a more carbanionic transition state, to increase the curvature. Consistent with this prediction is the excellent linearity in the plot of $|\tau|$ against ρ_H values (Fig. 4).

The positive deviation of the $|\tau|$ value for **1** from the plot in Fig. 4 may be because the transition state is closer to the E2–E1cb borderline. It was previously reported that the R_2NH-promoted eliminations from *p*-nitrophenyl *p*-nitrophenylacetate in MeCN proceeded by the E2–E1cb borderline mechanism, whereas the slightly less reactive *p*-nitrophenyl *m*-nitrophenylacetate reacted by the E2 mechanism.[14] If the position of the transition state for **1** is located very close to the E2–E1cb borderline, the susceptibility of the transition state charge character to the electron-withdrawing substituent, $|\tau|$, could be greater than predicted from the ρ_H value and show a positive deviation.

In conclusion, the ketene-forming eliminations from **1**–**5** promoted by R_2NH in MeCN proceed by the E2 mechanism *via* the E1cb-like transition state. The downward curvature observed in the Hammett plots appears to be due to the highly carbanionic transition state, which is moved towards the reactant on the horizontal reaction coordinate by a stronger electron-withdrawing substituent. It should be noted that concave upward Hammett plots were observed in elimination reactions that proceed *via* the E1-like transition state. The opposite curvatures observed for these two extremes in the spectrum of the variable E2 transition state seem to have a common origin, *i.e.*, the change in the charge character of the E2 transition state.

Experimental

Materials

4-Nitrophenyl arylacetates (**1a**–**d**) and 2,4-dinitrophenyl arylacetates (**5a**–**d**) were available from previous work. Other aryl arylacetates **2**–**4** were prepared from arylacetic acid and substituted phenols in the presence of Et_3N and 2-chloro-*N*-methylpyridinium iodide as previously reported.[14,19] Acetonitrile was purified, and solutions of R_2NH in MeCN were prepared as described before.[14] The yield (%), melting point (°C), IR (KBr, C=O, cm^{-1}), NMR (300 MHz, $CDCl_3$), and combustion analysis data for the compounds are as follows. Chemical shifts are in ppm and *J* values in Hz.

2-Methoxy-4-nitrophenyl phenylacetate (2a). Yield 42%; mp 41 °C; IR 1757; NMR δ 3.85 (s, 3H), 3.92 (s, 2H), 7.16 (d, 1H, $J = 8.6$), 7.35 (m, 5H), 7.81 (d, 1H, $J = 2.7$), 7.85 (dd, 1H, $J = 2.7, 8.6$); Anal. Calcd for $C_{15}H_{13}NO_5$: C, 62.72; H, 4.56; N, 4.88. Found: C, 62.96; H, 4.58; N, 4.86%.

2-Methoxy-4-nitrophenyl *p*-methoxyphenylacetate (2b). Yield 79%; mp 86 °C; IR 1778; NMR δ 3.82 (s, 3H), 3.86 (s, 2H), 3.87 (s, 3H), 6.91 (d, 2H, $J = 8.9$), 7.15 (d, 1H, $J = 8.7$), 7.30 (d, 2H, $J = 8.9$), 7.81 (d, 1H, $J = 2.4$), 7.86 (dd, 1H, $J = 2.4, 8.7$); Anal. Calcd for $C_{16}H_{15}NO_6$: C, 60.56; H, 4.77; N, 4.42. Found: C, 60.54; H, 4.78; N, 4.39%.

2-Methoxy-4-nitrophenyl *m*-chlorophenylacetate (2c). Yield 32%; mp oil; IR 1769; NMR δ 3.89 (s, 3H), 3.90 (s, 2H), 7.18 (d, 1H, $J = 8.7$), 7.29 (m, 3H), 7.43 (s, 1H), 7.82 (d, 1H, $J = 2.4$), 7.87 (dd, 1H, $J = 2.4, 8.7$); Anal. Calcd for $C_{15}H_{12}ClNO_5$: C, 55.99; H, 3.76; N, 4.35. Found: C, 55.92; H, 3.75; N, 4.32%.

2-Methoxy-4-nitrophenyl *m*-nitrophenylacetate (2d). Yield 67%; mp 61 °C; IR 1767; NMR δ 3.90 (s, 3H), 4.05 (s, 2H), 7.20 (d, 1H, $J = 8.9$), 7.58 (t, 1H, $J = 7.9$), 7.73 (d, 1H, $J = 7.9$), 7.84 (d, 1H, $J = 2.4$), 7.89 (dd, 1H, $J = 2.4, 8.9$), 8.21 (d, 1H, $J = 7.9$), 8.32 (s, 1H); Anal. Calcd for $C_{15}H_{12}N_2O_7$: C, 54.22; H, 3.64; N, 8.43. Found: C, 54.24; H, 3.67; N, 8.43%.

2-Chloro-4-nitrophenyl phenylacetate (3a). Yield 41%; mp 37 °C; IR 1768; NMR δ 3.96 (s, 2H), 7.33 (m, 6H), 8.15 (dd, 1H, $J = 2.6, 8.7$), 8.33 (d, 1H, $J = 2.6$); Anal. Calcd for $C_{14}H_{10}ClNO_4$: C, 57.65; H, 3.46; N, 4.80. Found: C, 57.71; H, 3.47; N, 4.79%.

2-Chloro-4-nitrophenyl *p*-methoxyphenylacetate (3b). Yield 54%; mp 98 °C; IR 1765; NMR δ 3.75 (s, 3H), 3.82 (s, 2H), 6.84 (d, 2H, $J = 8.4$), 7.22 (m, 3H), 7.24 (d, 2H, $J = 8.4$), 8.08 (dd, 1H, $J = 2.1, 8.7$), 8.27 (d, 1H, $J = 2.1$); Anal. Calcd for $C_{14}H_{10}ClNO_4$: C, 55.99; H, 3.76; N, 4.35. Found: C, 56.11; H, 3.78; N, 4.37%.

2-Chloro-4-nitrophenyl *m*-chlorophenylacetate (3c). Yield 40%; mp 68 °C; IR 1779; NMR δ 3.95 (s, 2H), 7.29 (m, 4H), 7.40 (s, 1H), 8.17 (dd, 1H, $J = 2.4, 8.7$), 8.35 (d, 1H, $J = 2.4$); Anal. Calcd for $C_{14}H_9Cl_2NO_4$: C, 51.54; H, 2.78; N, 4.29. Found: C, 51.59; H, 2.79; N, 4.27%.

2-Chloro-4-nitrophenyl *m*-nitrophenylacetate (3d). Yield 44%; mp 86 °C; IR 1765; NMR δ 4.10 (s, 2H), 7.36 (d, 1H, $J = 9.0$), 7.59 (t, 1H, $J = 8.1$), 7.75 (d, 1H, $J = 8.1$), 8.20 (m, 2H), 8.30 (s, 1H), 8.35 (d, 1H, $J = 2.1$); Anal. Calcd for $C_{14}H_9ClN_2O_6$: C, 49.93; H, 2.69; N, 8.32. Found: C, 49.77; H, 2.70; N, 8.28%.

4-Nitro-2-(trifluoromethyl)phenyl phenylacetate (4a). Yield 30%; mp 35 °C; IR 1755; NMR δ 3.95 (s, 2H), 7.36 (m, 5H), 7.47 (d, 1H, $J = 8.9$), 8.44 (dd, 1H, $J = 2.7, 8.9$), 8.57 (d, 1H, $J = 2.7$); Anal. Calcd for $C_{15}H_{10}F_3NO_4$: C, 55.39; H, 3.10; N, 4.31. Found: C, 55.34; H, 3.11; N, 4.33%.

4-Nitro-2-(trifluoromethyl)phenyl *p*-methoxyphenylacetate (4b). Yield 65%; mp 58 °C; IR 1779; NMR δ 3.82 (s, 3H), 3.88 (s, 2H), 6.91 (d, 2H, $J = 8.4$), 7.28 (d, 2H, $J = 8.4$), 7.45 (d, 1H,

$J = 9.0$), 8.43 (dd, 1H, $J = 2.4$, 9.0), 8.56 (d, 1H, $J = 2.4$); Anal. Calcd for $C_{16}H_{12}F_3NO_5$: C, 54.09; H, 3.40; N, 3.94. Found: C, 54.12; H, 3.41; N, 3.93%.

4-Nitro-2-(trifluoromethyl)phenyl *m*-chlorophenylacetate (4c). Yield 24%; mp oil; IR 1767; NMR δ 3.98 (s, 2H), 7.34 (m, 3H), 7.37 (s, 1H), 7.48 (d, 1H, $J = 8.7$), 8.45 (dd, 1H, $J = 2.7$, 8.7), 8.58 (d, 1H, $J = 2.7$); Anal. Calcd for $C_{15}H_9ClF_3NO_4$: C, 50.08; H, 2.52; N, 3.89. Found: C, 50.19; H, 2.53; N, 3.91%.

4-Nitro-2-(trifluoromethyl)phenyl *m*-nitrophenylacetate (4d). Yield 45%; mp 69 °C; IR 1771; NMR δ 4.08 (s, 2H), 7.51 (d, 1H, $J = 8.9$), 7.59 (t, 1H, $J = 8.3$), 7.71 (d, 1H, $J = 8.3$), 8.23 (d, 1H, $J = 8.3$), 8.26 (s, 1H), 8.47 (dd, 1H, $J = 2.7$, 8.9), 8.58 (d, 1H, $J = 2.7$); Anal. Calcd for $C_{15}H_9F_3N_2O_6$: C, 48.66; H, 2.45; N, 7.57. Found: C, 48.63; H, 2.43; N, 7.60%.

Kinetic studies

Reactions of **2**–**4** with R_2NH in MeCN were followed by monitoring the increase in the absorbance of the aryl oxides at 400–450 nm with a UV–vis spectrophotometer as described before.[14]

Product studies

When the reactions of **2**–**4** with R_2NH in MeCN were monitored periodically with reaction time, the absorbance corresponding to the reactant at 260–280 nm decreased, while that for the aryl oxides increased at 400–450 nm. In all cases clean isosbestic points were observed at 292–298 nm. The yields of the aryl oxides, determined by comparing the absorbance of the infinity samples from the kinetic reactions with those of authentic aryl oxides, were in the range 90–98%.

Control experiments

The stabilities of **2**–**4** were determined as reported earlier.[14] They were stable for at least 3 weeks in MeCN solution at room temperature.

Acknowledgements

This research was supported by the BK21 program (Korea Ministry of Education), CRM-KOSEF, and the National Research Laboratory Program (Korea Ministry of Science and Technology).

References

1 B. Holomquist and T. C. Bruice, *J. Am. Chem. Soc.*, 1969, **91**, 2993.
2 B. Holomquist and T. C. Bruice, *J. Am. Chem. Soc.*, 1969, **91**, 3003.
3 R. F. Pratt and T. C. Bruice, *J. Am. Chem. Soc.*, 1970, **92**, 5956.
4 M. Inoue and T. C. Bruice, *J. Am. Chem. Soc.*, 1982, **104**, 1644.
5 M. Inoue and T. C. Bruice, *J. Org. Chem.*, 1982, **47**, 959.
6 A. William, *J. Chem. Soc.*, *Perkin Trans. 2*, 1972, 808.
7 A. William and K. T. Douglas, *Chem. Rev.*, 1975, 627.
8 W. Tagaki, S. Kobayashi, K. Kurihara, K. Kurashima, Y. Yoshida and J. Yano, *J. Chem. Soc.*, *Chem. Commun.*, 1976, 843.
9 T. J. Broxton and N. W. Duddy, *J. Org. Chem.*, 1981, **46**, 1186.
10 R. Chandrasekar and N. Venkatasubramanian, *J. Chem. Soc.*, *Perkin Trans. 2*, 1982, 1625.
11 K. T. Douglas, M. Alborz, G. R. Rullo and N. F. Yaggi, *J. Chem. Soc.*, *Chem. Commun.*, 1982, 242.
12 N. S. Isaac and T. S. Najem, *J. Chem. Soc.*, *Perkin Trans. 2*, 1988, 557.
13 S. Y. Chung, S. D. Yoh, J. H. Choi and K. T. Shim, *J. Korean Chem. Soc.*, 1992, **36**, 446.
14 B. R. Cho, Y. K. Kim and C.-O. Maing Yoon, *J. Am. Chem. Soc.*, 1997, **119**, 691.
15 B. R. Cho, Y. K. Kim, J. S. Yoon, J. C. Kim and S. Y. Pyun, *J. Org. Chem.*, 2000, **65**, 1239.
16 J. F. Bunnett, S. Sridharan and W. P. Cavin, *J. Org. Chem.*, 1979, **44**, 1458.
17 T. Hasan, L. B. Sim and A. Fry, *J. Am. Chem. Soc.*, 1983, **105**, 3967.
18 M. C. Cabaleiro and R. S. Montani, *J. Chem. Res.* (*S*), 1986, 220.
19 K. Saigo, M. Usui, K. Kikuchi, E. Shimada and T. Mukaiyama, *Bull. Chem. Soc. Jpn.*, 1977, **50**, 1863.
20 *MicroCal Origin Version 3.5*, MicroCal Software, Inc., Northampton, MA, 1991.
21 W. H. Saunders, Jr. and A. F. Cockerill, *Mechanism of Elimination Reactions*, Wiley, New York, 1973, pp. 510–523.
22 T. H. Lowry and K. S. Richardson, *Mechanism and Theory in Organic Chemistry*, Harper and Row, New York, 1987, pp. 591–616.
23 J. R. Gandler, in *The Chemistry of Double Bonded Functional Groups*, ed. S. Patai, John Wiley & Sons, Chichester, 1989, vol. 2, part 1, pp. 734–797.
24 W. P. Jencks, *Chem. Rev.*, 1985, **85**, 511.
25 R. V. Hoffman and E. L. Belfore, *J. Am. Chem. Soc.*, 1982, **104**, 2183.
26 W. Tagaki, S. Kobayashi, K. Kurihara, K. Kurashima, Y. Yoshida and J. Yanao, *J. Chem. Soc.*, *Chem. Commun.*, 1976, 843.
27 R. V. Hoffman and J. M. Shankweiler, *J. Am. Chem. Soc.*, 1986, **108**, 5536.
28 P. R. Young and W. P. Jencks, *J. Am. Chem. Soc.*, 1979, **101**, 3288.
29 R. S. Drago and J. A. Zoltewicz, *J. Org. Chem.*, 1994, **59**, 2824.
30 T. Yishida, Y. Yano and S. Oae, *Tetrahedron*, 1971, **27**, 5343.